力学与航空航天工程系

DEPARTMENT OF MECHANICS AND AEROSPACE ENGINEERING

SOUTHERN UNIVERSITY
OF SCIENCE AND TECHNOLOGY

Advanced Computational Fluid Dynamics Project

Student Names & IDs:

Weiyuan Liang – 12332535

Professor: *Prof. Wang*

Date: *June 19, 2024*

1. Question Description

Consider the forced Burgers equation

$$\frac{\partial u}{\partial t} + u\frac{\partial u}{\partial x} = \nu\frac{\partial^2 u}{\partial x^2} + f(x,t) \tag{1}$$

in a periodic domain of length $L = 1$ with the kinematic viscosity ν, where the flow velocity u is a function of x and t.
Initial condition:

$$u(x,t=0) = 0 \tag{2}$$

Steady forcing term:

$$f(x,t) = \frac{u_0^2}{L}\left[sin\left(\frac{2\pi x}{L}\right) + cos\left(\frac{4\pi x}{L}\right)\right] \tag{3}$$

2. Finite Differnece Method

2.1. Program build up

In this question, the computational domain is periodical and it is from 0 to 1. We add one virtual node on the last of the computational domain, plot the skretch of it as show as Fig.1

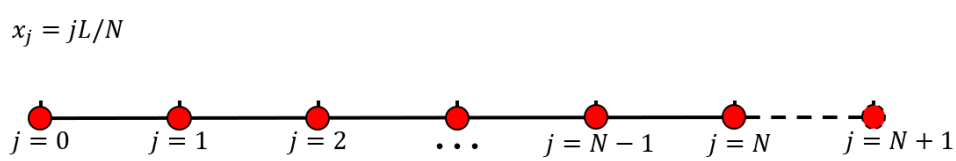

Figure 1. The mesh of finite differencing method with a virtual node on the right boundary.

All the spatial derivatives use the second central differencing, such that

$$\begin{aligned}\left(\frac{\partial u}{\partial x}\right)_j &= \frac{\delta u_j}{\delta x} = \frac{u_{j+1} - u_{j-1}}{\Delta x} \\ \left(\frac{\partial^2 u}{\partial x^2}\right)_j &= \frac{\delta^2 u_j}{\delta x^2} = \frac{u_{j+1} - 2u_j + u_{j-1}}{\Delta x^2}\end{aligned} \tag{4}$$

For the nonlinear term and forcing term, use the Adams-Bashforth scheme such that

$$\frac{u^{n+1} - u^n}{\Delta t} = \frac{3}{2}F(u^n) - \frac{1}{2}F(u^{n-1}) \tag{5}$$

For the viscous term, use the Crank-Nicholson scheme, such that

$$\frac{u^{n+1} - u^n}{\Delta t} = \frac{1}{2}F(u^{n+1}) + \frac{1}{2}F(u^n) \tag{6}$$

Subtitude all of the differencing scheme into the govern equation and make some rearrangement, yield the differencing equation:

$$
\begin{aligned}
& u_j^{n+1} - \frac{\nu \Delta t}{2(\Delta x)^2}(u_{j+1}^{n+1} - 2u_j^{n+1} + u_{j-1}^{n+1}) \\
= \quad & u_j^n - \frac{3}{2}\left(\frac{\Delta t}{2\Delta x}\right)\left[\left(\frac{u^2}{2}\right)_{j+1}^n - \left(\frac{u^2}{2}\right)_{j-1}^n\right] + \frac{1}{2}\left(\frac{\Delta t}{2\Delta x}\right)\left[\left(\frac{u^2}{2}\right)_{j+1}^{n-1} - \left(\frac{u^2}{2}\right)_{j-1}^{n-1}\right] \\
& + \frac{\nu \Delta t}{2(\Delta x)^2}(u_{j+1}^n - 2u_j^n + u_{j-1}^n) + \frac{(\Delta t)u_0^2}{L}\left[sin\left(\frac{2\pi x_j}{L}\right) + cos\left(\frac{4\pi x_j}{L}\right)\right]
\end{aligned} \tag{7}
$$

This is an implicit equation, we express it as the matrix form **Ax=b** like

$$
\begin{pmatrix}
1 & 0 & 0 & 0 & \cdots & 0 & -1 & 0 \\
-c & 1+2c & -c & 0 & \cdots & 0 & 0 & 0 \\
0 & -c & 1+2c & -c & \cdots & 0 & 0 & 0 \\
\vdots & & \ddots & \ddots & \ddots & & & \vdots \\
0 & 0 & 0 & 0 & \cdots & -c & 1+2c & -c \\
0 & -1 & 0 & 0 & \cdots & 0 & 0 & 1
\end{pmatrix}
\begin{pmatrix}
u_0^{n+1} \\ u_1^{n+1} \\ u_2^{n+1} \\ \vdots \\ u_N^{n+1} \\ u_{N+1}^{n+1}
\end{pmatrix}
=
\begin{pmatrix}
0 \\ u_1^n + H_1^n + V_1^n + F_1^n \\ u_2^n + H_2^n + V_2^n + F_2^n \\ \vdots \\ u_N^n + H_N^n + V_N^n + F_N^n \\ 0
\end{pmatrix} \tag{8}
$$

where $c = \frac{N\alpha}{2\mathrm{Re}}$, $\alpha = \frac{u_0 \Delta t}{\Delta x}$ is the CFL number and the terms in the R.H.S

$$
\begin{aligned}
H_j^n &= -\frac{3}{2}\left(\frac{\Delta t}{2\Delta x}\right)\left[\left(\frac{u^2}{2}\right)_{j+1}^n - \left(\frac{u^2}{2}\right)_{j-1}^n\right] + \frac{1}{2}\left(\frac{\Delta t}{2\Delta x}\right)\left[\left(\frac{u^2}{2}\right)_{j+1}^{n-1} - \left(\frac{u^2}{2}\right)_{j-1}^{n-1}\right] \\
V_j^n &= \frac{\nu \Delta t}{2(\Delta x)^2}(u_{j+1}^n - 2u_j^n + u_{j-1}^n) \\
F_j^n &= \frac{(\Delta t)u_0^2}{L}\left[sin\left(\frac{2\pi x_j}{L}\right) + cos\left(\frac{4\pi x_j}{L}\right)\right]
\end{aligned} \tag{9}
$$

The coefficient matrix **A** is a $(N+2)\times(N+2)$ order matrix, we can ruduce it to a $N \times N$ matrix like

$$
\mathbf{A} = \begin{pmatrix}
1+2c & -c & 0 & \cdots & 0 & -c \\
-c & 1+2c & -c & \cdots & 0 & 0 \\
\vdots & \ddots & \ddots & \ddots & & \vdots \\
-c & 0 & 0 & \cdots & -c & 1+2c
\end{pmatrix} \tag{10}
$$

We reduce the computational cost by this procedure, and we just need calculate u for $x1$ to x_N. The value of u_0 and u_{N+1} can be obtained by the periodic boundary condition.

This matrix is solved by tri-diag subrutine with a periodical condition. And the numerical integral in this program use the the Trapezoidal rule.

2.2. Result

The procedure we decide the mesh resolution which need to obtain the converged numerical solution is checking whether $P - \varepsilon \to 0$. For Reynolds number $Re = 1000$, CFL number $\alpha = 0.325$,

we choose resolutio $N = 3200$ as the benchmark to calculate the normalized L1 and L2 error. As shown as Fig.2, the accuracy in this numerical method is second order.

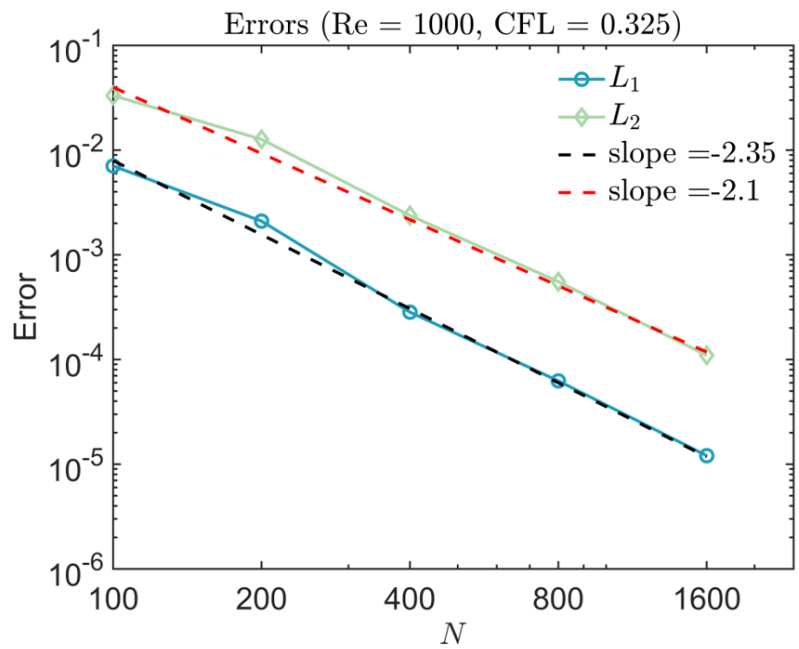

Figure 2. The normalized error of Finite Differnece Method

To evaluate how the solution evolue in time, we devided into 4 stages: 1) Initial stage; 2) The first discontinuity arise; 3) The second discontinuity arise; 4) Two discontinuity meger to one biggest one. We choose one specific time in each stage(i.e. $\tilde{t} = u_0 t / L = 0.25, 0.50, 1.00, 2.00$), plot the velocity distribution as show as Fig.3

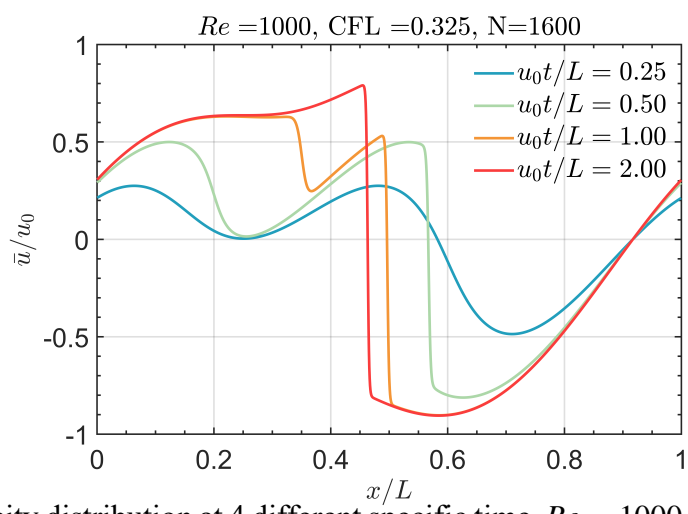

Figure 3. The velocity distribution at 4 different specific time, $Re = 1000, CFL = 0.325, N = 1600$

To evaluate how the spatial averaged terms evolue in time, we calcualte the average kinetic energy $ke = \left\langle \frac{u^2}{2} \right\rangle$, the average viscous dissipation rate $\varepsilon = \nu \left\langle (\frac{\partial u}{\partial x})^2 \right\rangle$, and the rate of energy input

by the forcing term $P = \langle f(x) \cdot u(x,t) \rangle$, which $\langle\rangle$ represent the spatial averaged procedure. The result as shown as Fig.4, it shows that the average kinetic energy and the rate of energy input by the forcing term is nearly same, but the average viscous dissipation rate is different. When N is relatively small, there are some oscillation on the curve of dissipation rate.

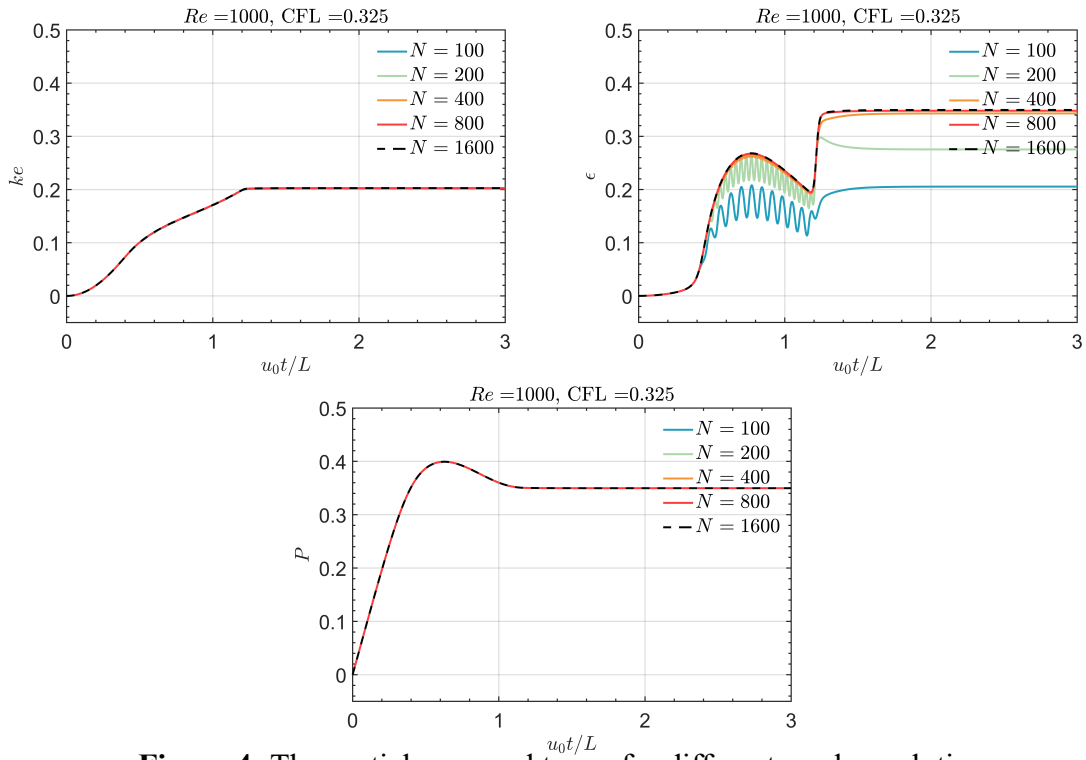

Figure 4. The spatial averaged terms for different mesh resolution

3. Finite Volume Method

3.1. Program build up

Diffustion flux:
The original equation is :

$$\frac{\partial u}{\partial t} + u\frac{\partial u}{\partial x} = v\frac{\partial^2 u}{\partial x^2} + f(x,t) \tag{11}$$

The discrete equation can be derived as :

$$\frac{d}{dt}\bar{u}_j + \frac{1}{\Delta x}\left(\hat{f}_{j+0.5} - \hat{f}_{j-0.5}\right) = \frac{1}{\Delta x}\left(\hat{D}_{j+0.5} - \hat{D}_{j-0.5}\right) + \bar{f}_j \tag{12}$$

Firstly, we consider the diffusion term. We obtain the diffusion flux $\hat{D}_{j+0.5}$, by reconstruction based on a 4 points stencil $\{\bar{u}_{j-1}, \bar{u}_j, \bar{u}_{j+1}, \bar{u}_{j+2}\}$. P^3: $u(\xi) = a\xi^3 + b\xi^2 + c\xi + d$, where $\xi = x - x_j$.

$$\begin{aligned}
\int_{x=x_j-\frac{3}{2}\Delta x}^{x=x_j-\frac{1}{2}\Delta x} p_3 dx &= \bar{u}_{j-1} \\
\int_{x=x_j-\frac{1}{2}\Delta x}^{x=x_j+\frac{1}{2}\Delta x} p_3 dx &= \bar{u}_j \\
\int_{x=x_j+\frac{1}{2}\Delta x}^{x=x_j+\frac{3}{2}\Delta x} p_3 dx &= \bar{u}_{j+1} \\
\int_{x=x_j+\frac{3}{2}\Delta x}^{x=x_j+\frac{5}{2}\Delta x} p_3 dx &= \bar{u}_{j+2}
\end{aligned} \tag{13}$$

$$\begin{aligned}
a &= \frac{\bar{u}_{j+2} - 3\bar{u}_{j+1} + 3\bar{u}_j - \bar{u}_{j-1}}{6\Delta x^3} \\
b &= \frac{\bar{u}_{j+1} - 2\bar{u}_j + \bar{u}_{j-1}}{2\Delta x^2} \\
c &= \frac{-5\bar{u}_{j+2} + 27\bar{u}_{j+1} - 15\bar{u}_j - 7\bar{u}_{j-1}}{24\Delta x} \\
d &= \frac{-\bar{u}_{j+1} + 26\bar{u}_j - \bar{u}_{j-1}}{24\Delta x}
\end{aligned} \tag{14}$$

Combined with Taylor expansion:

$$\begin{aligned}
\bar{u}_{j+2} &= u_j + 2u'_j\Delta x + \frac{49}{24}u''_j\Delta x^2 + \frac{17}{12}u'''_j\Delta x^3 \\
\bar{u}_{j+1} &= u_j + u'_j\Delta x + \frac{13}{24}u''_j\Delta x^2 + \frac{5}{24}u'''_j\Delta x^3 \\
\bar{u}_j &= u_j + \frac{1}{24}u''_j\Delta x^2 \\
\bar{u}_{j-1} &= u_j - u'_j\Delta x + \frac{13}{24}u''_j\Delta x^2 - \frac{5}{24}u'''_j\Delta x^3
\end{aligned} \tag{15}$$

Then we know that $\frac{\partial u}{\partial x} = 3a\xi^2 + 2b\xi + c$, so:

$$\begin{aligned} \left.\frac{\partial u}{\partial x}\right|_{\eta=\frac{1}{2}\Delta x} &= \frac{-\overline{u}_{j+2} + 15\overline{u}_{j+1} - 15\overline{u}_j + \overline{u}_{j-1}}{12\Delta x} \\ \hat{D}_{j+1/2} = \nu \left.\frac{\partial u}{\partial x}\right|_{\eta=j+0.5} &= \frac{\nu}{12\Delta x}\left(\overline{u}_{j-1} - 15\overline{u}_j + 15\overline{u}_{j+1} - \overline{u}_{j+2}\right) \end{aligned} \tag{16}$$

Combine with equation (7):

$$\left.\frac{\partial u}{\partial x}\right|_{\xi=\frac{1}{2}\Delta x} = u'_j + \frac{1}{2}u''_j(\Delta x) + \frac{1}{8}u_j^{(3)}(\Delta x)^2 + \frac{1}{48}u_j^{(4)}(\Delta x)^3 - \frac{49}{5760}u_j^{(5)}(\Delta x)^4 \tag{17}$$

In Taylor expansion:

$$\left.\frac{\partial u}{\partial x}\right|_{\xi=\frac{1}{2}\Delta x} = u'_j + \frac{1}{2}u''_j(\Delta x) + \frac{1}{8}u_j^{(3)}(\Delta x)^2 + \frac{1}{48}u_j^{(4)}(\Delta x)^3 + \frac{1}{3840}u_j^{(5)}(\Delta x)^4 \tag{18}$$

Consequently, the leading order term is fourth order.

Viscous term

For viscous term, we use fifth order WENO to reconstruct function, then using Lax-Fredrich flux format.Reconstruction:

$$\begin{aligned} u_{j+0.5}^{+(5)} &= \omega_1 u_{j+0.5}^{(1)} + \omega_2 u_{j+0.5}^{(2)} + \omega_3 u_{j+0.5}^{(3)} \\ u_{j+0.5}^{-(5)} &= \omega_1 u_{j+0.5}^{(1)} + \omega_2 u_{j+0.5}^{(2)} + \omega_3 u_{j+0.5}^{(3)} \end{aligned} \tag{19}$$

Reconstruct the polynomial of P(1) P(2) P(3) And let $x = x_j + 0.5\Delta x$, we can get the stencil for $u_{j+0.5}^{(1)}$,$u_{j+0.5}^{(2)}$, $u_{j+0.5}^{(3)}$, in positive direction in $I_{j-1}, I_j, Ij+1, I_{j+2}, I_{j+3}$ that is:

$$\begin{aligned} u_{j+0.5}^{(1)} &= \frac{1}{3}\overline{u}_{j+1} + \frac{5}{6}\overline{u}_j - \frac{1}{6}\overline{u}_{j-1} \\ u_{j+0.5}^{(2)} &= -\frac{1}{6}\overline{u}_{j+2} + \frac{5}{6}\overline{u}_{j+1} + \frac{1}{3}\overline{u}_j \\ u_{j+0.5}^{(3)} &= \frac{1}{3}\overline{u}_{j+3} - \frac{7}{6}\overline{u}_{j+2} + \frac{11}{6}\overline{u}_{j+1} \end{aligned} \tag{20}$$

Then

$$\begin{aligned} \beta_1 &= \frac{13}{12}\left(\bar{u}_{j-1} - 2\bar{u}_j + \bar{u}_{j+1}\right)^2 + \frac{1}{4}\left(\bar{u}_{j-1} - 4\bar{u}_j + 3\bar{u}_{j+1}\right)^2 \\ \beta_2 &= \frac{13}{12}\left(\bar{u}_j - 2\bar{u}_{j+1} + \bar{u}_{j+2}\right)^2 + \frac{1}{4}\left(\bar{u}_j - \bar{u}_{j+2}\right)^2 \\ \beta_3 &= \frac{13}{12}\left(\bar{u}_{j+1} - 2\bar{u}_{j+2} + \bar{u}_{j+3}\right)^2 + \frac{1}{4}\left(3\bar{u}_{j+1} - 4\bar{u}_{j+2} + \bar{u}_{j+3}\right)^2 \end{aligned} \tag{21}$$

which $\gamma_1 = 3/10$; $\gamma_2 = 3/5$; $\gamma_3 = 1/10$; $\omega_n = \frac{\tilde{\omega}_n}{\tilde{\omega}_1 + \tilde{\omega}_2 + \tilde{\omega}_3}$ with $\tilde{\omega}_\alpha = \frac{\gamma_\alpha}{(\varepsilon + \beta_\alpha)^2}$

Reconstruct the polynomial of P(1) P(2) P(3) And let $x = x_j + 0.5\Delta x$, we can get the stencil for $u_{j+0.5}^{(1)}$,$u_{j+0.5}^{(2)}$, $u_{j+0.5}^{(3)}$, in negative direction in $I_{j-2}, I_{j-1}, Ij, I_{j+1}, I_{j+2}$ that is:

$$
\begin{aligned}
u^{(1)}_{j+0.5} &= \frac{11}{6}\bar{u}_j - \frac{7}{6}\bar{u}_{j-1} - \frac{1}{3}\bar{u}_{j-2} \\
u^{(2)}_{j+0.5} &= -\frac{1}{3}\bar{u}_{j+1} + \frac{5}{6}\bar{u}_j - \frac{1}{6}\bar{u}_{j-1} \\
u^{(3)}_{j+0.5} &= -\frac{1}{6}\bar{u}_{j+2} - \frac{5}{6}\bar{u}_{j+1} + \frac{1}{3}\bar{u}_j
\end{aligned} \tag{22}
$$

Then

$$
\begin{aligned}
\beta_1 &= \frac{13}{12}\left(\bar{u}_{j-2} - 2\bar{u}_{j-1} + \bar{u}_j\right)^2 + \frac{1}{4}\left(\bar{u}_{j-2} - 4\bar{u}_{j-1} + 3\bar{u}_j\right)^2 \\
\beta_2 &= \frac{13}{12}\left(\bar{u}_{j-1} - 2\bar{u}_j + \bar{u}_{j+1}\right)^2 + \frac{1}{4}\left(\bar{u}_{j-1} - \bar{u}_{j+1}\right)^2 \\
\beta_3 &= \frac{13}{12}\left(\bar{u}_j - 2\bar{u}_{j+1} + \bar{u}_{j+2}\right)^2 + \frac{1}{4}\left(3\bar{u}_j - 4\bar{u}_{j+1} + \bar{u}_{j+2}\right)^2
\end{aligned} \tag{23}
$$

which $\gamma_1 = 1/10$; $\gamma_2 = 3/5$; $\gamma_3 = 3/10$; $\omega_n = \frac{\tilde{\omega}_n}{\tilde{\omega}_1+\tilde{\omega}_2+\tilde{\omega}_3}$ with $\tilde{\omega}_\alpha = \frac{\gamma_\alpha}{(\varepsilon+\beta_\alpha)^2}$ Use Lax-Fredrich flux format:

$$
\hat{f}_{j+0.5} = \hat{f}(u^-_{j+0.5}, u^+_{j+0.5}) = \frac{1}{2}\left[f(u^-_{j+0.5}) + f(u^+_{j+0.5})\right] - \alpha(u^+_{j+0.5} - u^-_{j+0.5}) \tag{24}
$$

where $\alpha = \max|\hat{f}'(u)|$, $f(u) = \frac{1}{2}u^2$.

Forcing term

$$
\overline{f}_j = \int_{x_{j-0.5}}^{x_{j+0.5}} f(x,t)\,dx = \frac{u_0^2}{L}\left[\sin\left(\frac{2\pi x_j}{L}\right)\cdot\frac{\sin(\pi\Delta x/L)}{\pi\Delta x/L} + \cos\left(\frac{4\pi x_j}{L}\right)\cdot\frac{\cos(2\pi\Delta x/L)}{2\pi\Delta x/L}\right] \tag{25}
$$

Time iteration

For time iteration we use third order Rungle - Kutta method:

$$
\begin{aligned}
F(u) = -\frac{1}{\Delta x}(\hat{f}_{j+0.5} - \hat{f}_{j-0.5}) + \frac{1}{\Delta x}(\hat{D}_{j+0.5} - \hat{D}_{j-0.5}) + \overline{f}_j \\
u^{(1)} = u^n + \Delta t\, F(u^n) \\
u^{(2)} = u^n + \Delta t\left(\frac{1}{4}F(u^n) + \frac{1}{4}F(u^{(1)})\right) \\
u^{(n+1)} = u^n + \Delta t\left(\frac{1}{6}F(u^n) + \frac{2}{3}F(u^{(2)}) + \frac{1}{6}F(u^{(1)})\right)
\end{aligned} \tag{26}
$$

Mesh

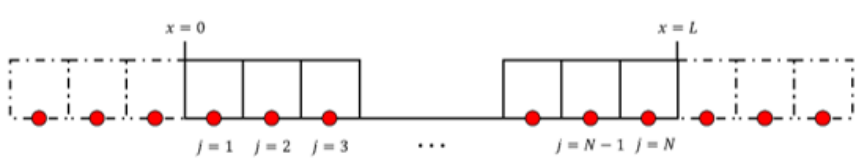

Figure 5. The mesh set up in FVM

3.2. Result

With the smae postprocess of part.1, we use $Re = 3200$ as the benchmark, and calcualte the L1 and L2 error of local value. The result as shown in Fig.6, it shows that the slope is nearly equal to -3. The spatial averaged term as shown in Fig.7.

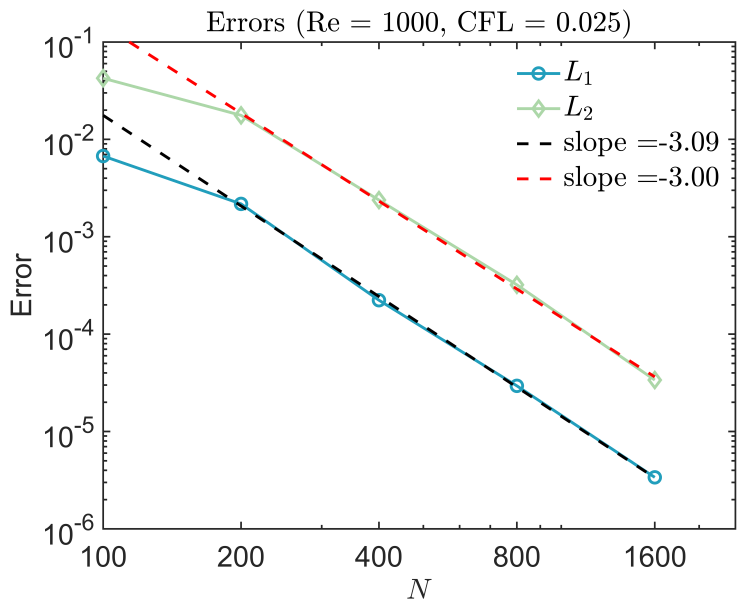

Figure 6. The normalized Error in FVM

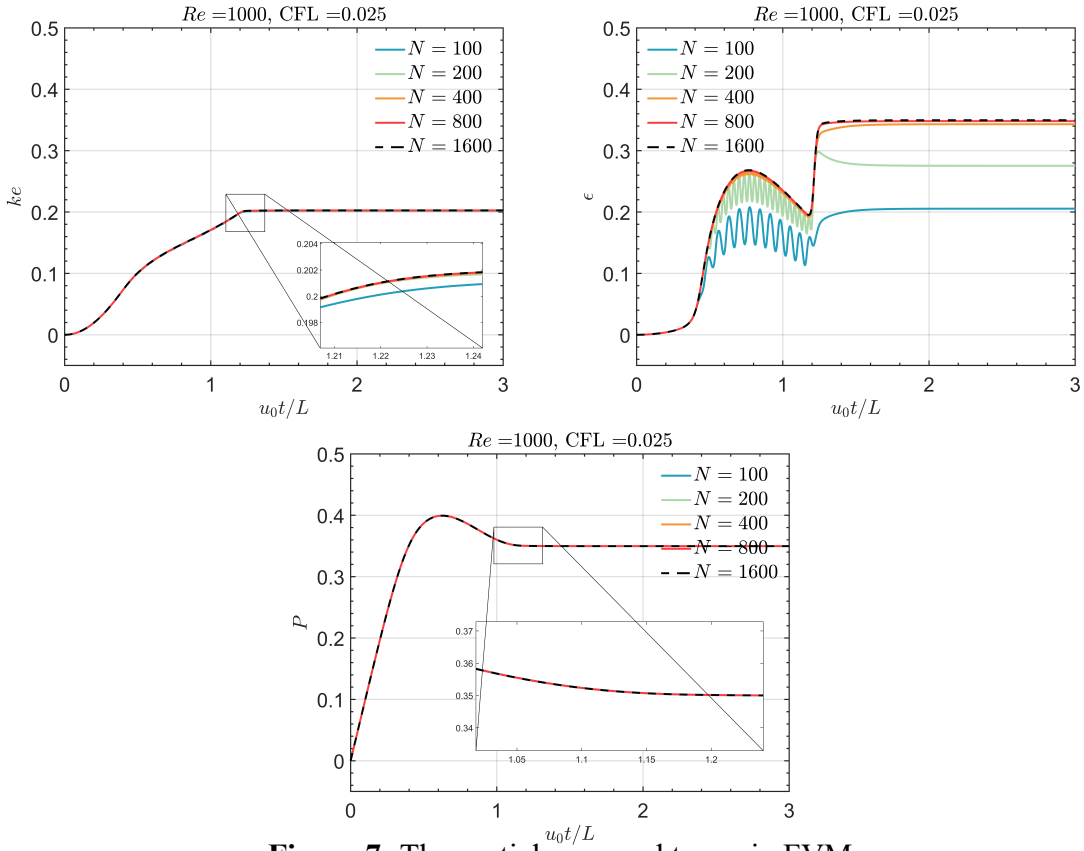

Figure 7. The spatial averaged terms in FVM

4. Physical Problem Discussion

4.1. Stability judgement

To evaluate the grid resolution we need to obtain the accurate numerical solution in Finite difference method, we increase the mesh solution from small to large at the fixed Re, and check $P - \varepsilon_{FFT}$ at $\tilde{t} = u_0 L/L = 3.2$ whether smaller than $4e-3$. And ε_{FFT} represent the averaged dissipation rate calcualted by Fast Fourier Transform(FFT). The result as shown as Fig.8. When $Re \leq 4000$, the slope of the boundary line between accuracy region and inaccuracy region is nearly equal to 1; when $RE > 4000$, the symbol shows a exponential increasing trend.

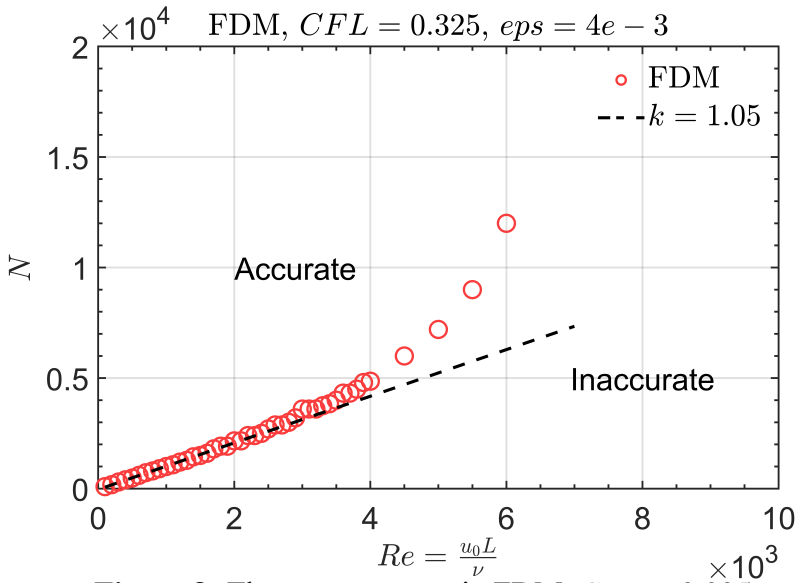

Figure 8. The accurate map in FDM, $CFL = 0.325$

Due to FVM is sentisive to CFL number, we plot the stability map for different Re as shown as Fig.9. The left lower region is unstable, right upper region is stable. With the increased Re, the unstable region is becoming larger. If we plot the log-log figure, we can see that their slope is -1 and the interval between two line is same. When the Re is large (e.g. $Re \geq 1600$), there is a maximum CFL number in stability map.

4.2. Spatial terms for differnet Reynolds numbers

The spatial terms for different Reynolds numbers in FDM and FVM as shown as Fig.10 and Fig.11. Higher Re values tend to have a slightly higher kinetic energy at steady state.As the Re increases, the slope of ε at the turning point becomes steeper and steeper. For lower Re values (e.g. $Re = 100, 200$), P reaches a lower steady-state value compared to higher Re values.

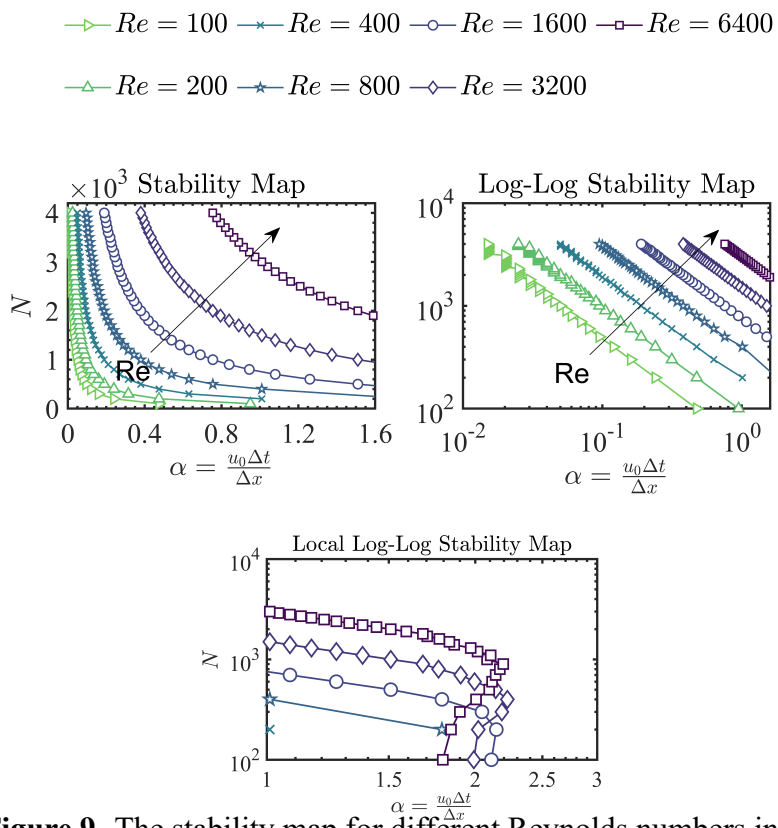

Figure 9. The stability map for different Reynolds numbers in FVM

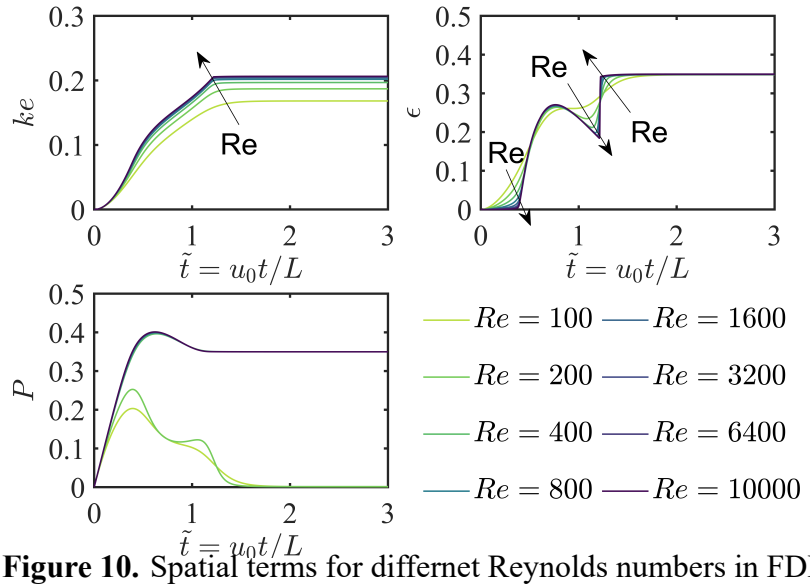

Figure 10. Spatial terms for differnet Reynolds numbers in FDM

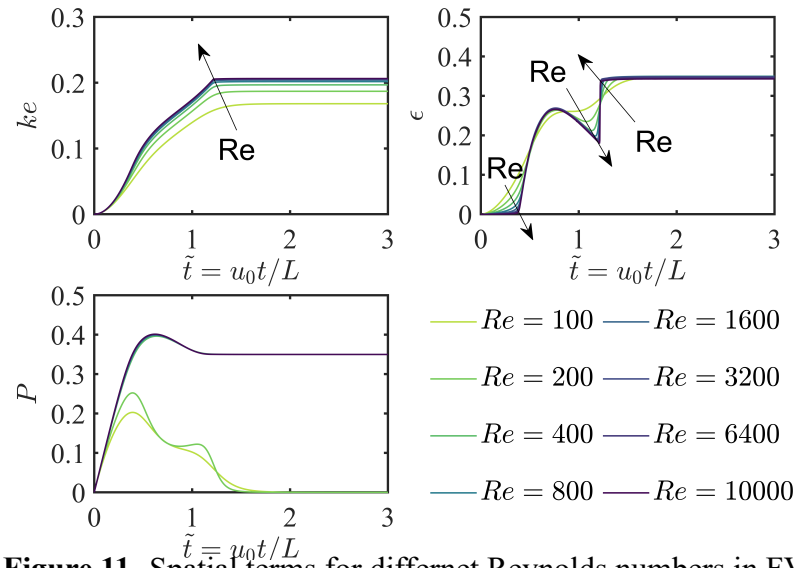

Figure 11. Spatial terms for differnet Reynolds numbers in FVM

4.3. velocity distribution for differnet Reynolds numbers

In Fig.12 and Fig.13, we can see that, with the increased Reynolds number, the discontinuity get steeper and steeper.

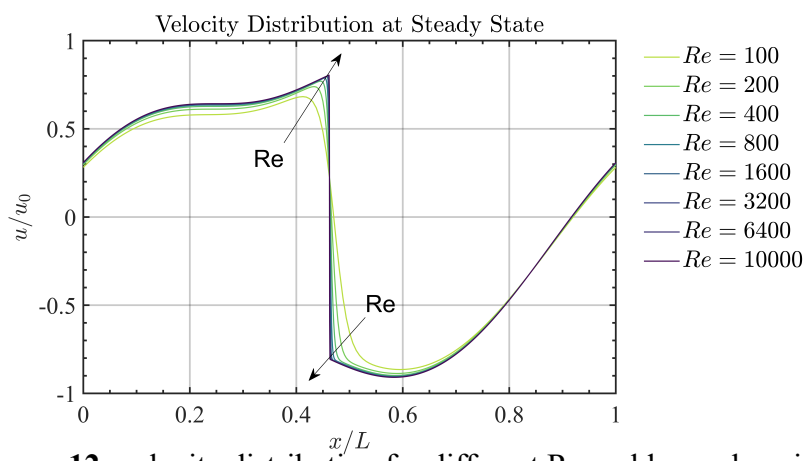

Figure 12. velocity distribution for differnet Reynolds numbers in FDM

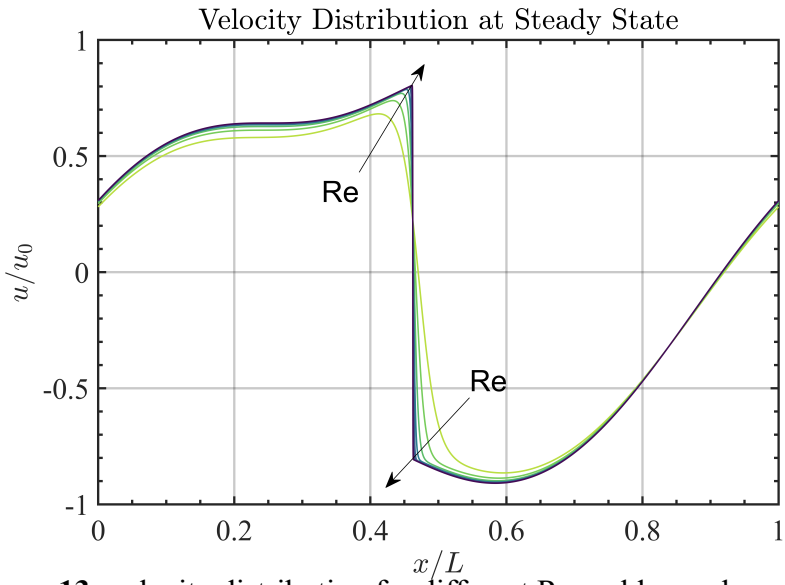

Figure 13. velocity distribution for differnet Reynolds numbers in FVM

4.4. Energy Spectrum for differnet Reynolds numbers

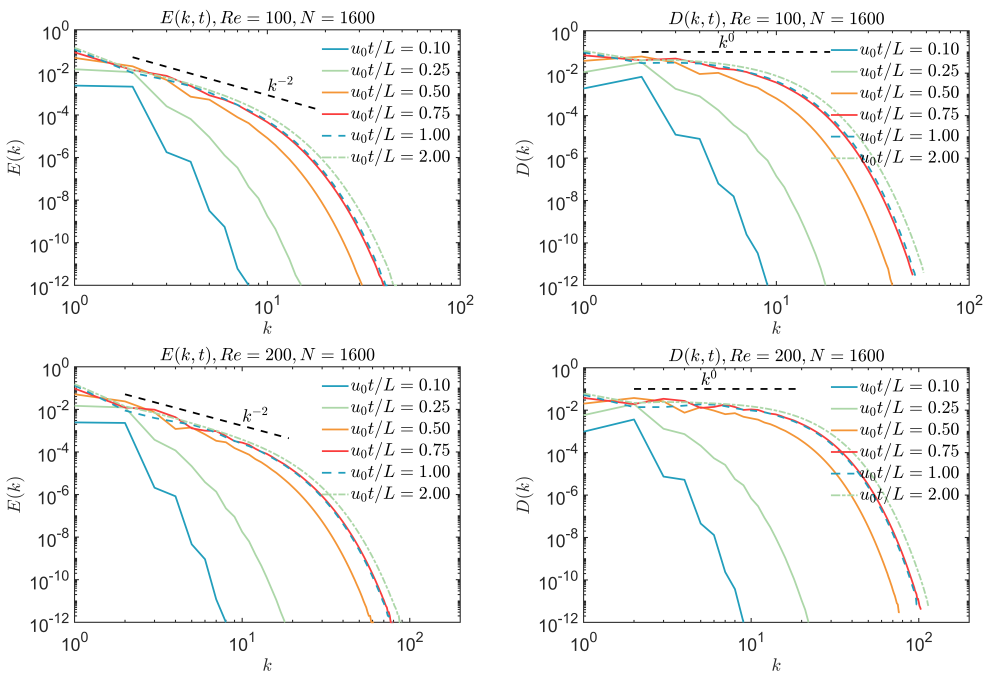

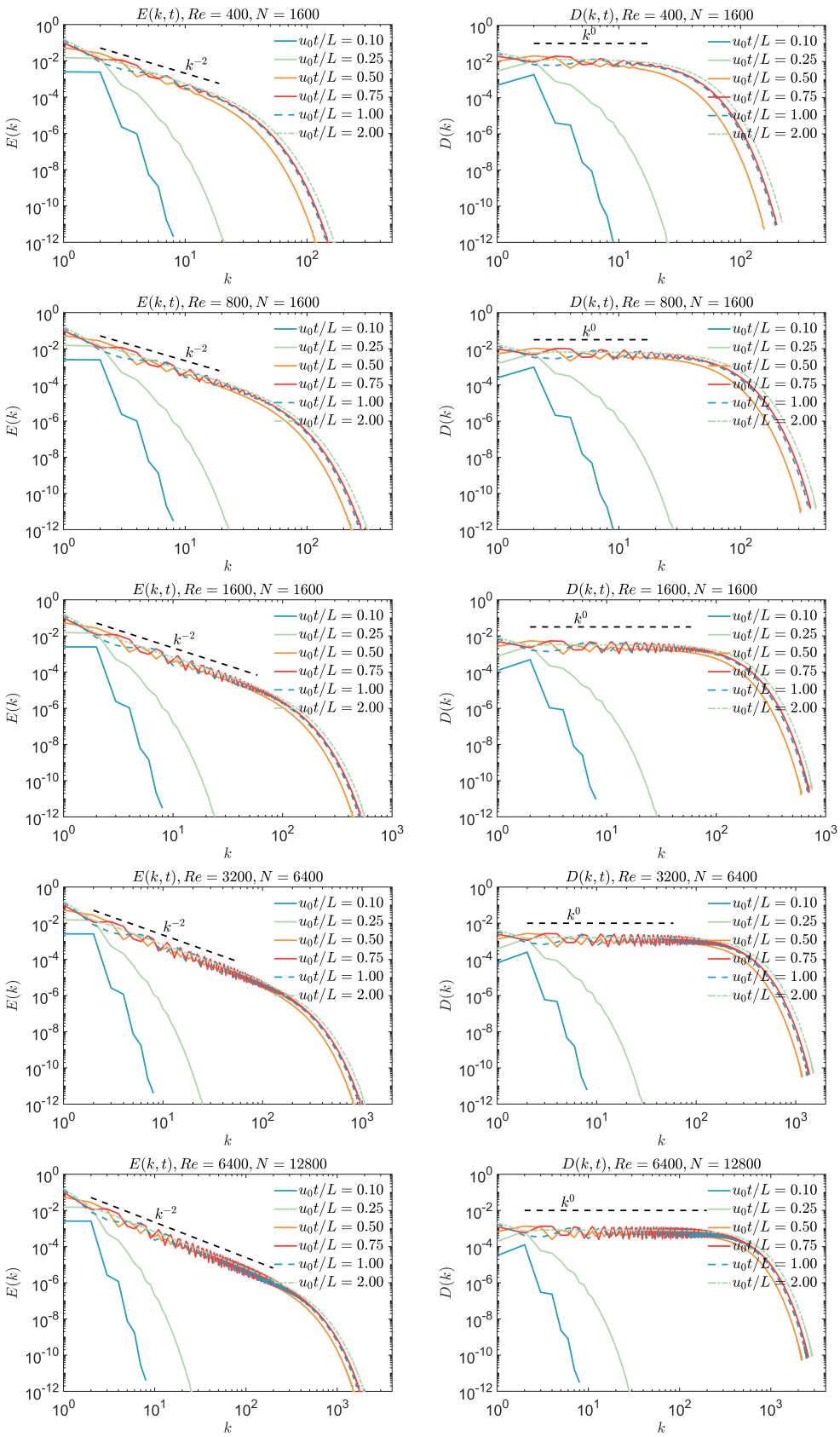
$E(k,t), Re = 400, N = 1600$
$D(k,t), Re = 400, N = 1600$
$E(k,t), Re = 800, N = 1600$
$D(k,t), Re = 800, N = 1600$
$E(k,t), Re = 1600, N = 1600$
$D(k,t), Re = 1600, N = 1600$
$E(k,t), Re = 3200, N = 6400$
$D(k,t), Re = 3200, N = 6400$
$E(k,t), Re = 6400, N = 12800$
$D(k,t), Re = 6400, N = 12800$
k^{-2}
k^{0}
$u_0t/L = 0.10$
$u_0t/L = 0.25$
$u_0t/L = 0.50$
$u_0t/L = 0.75$
$u_0t/L = 1.00$
$u_0t/L = 2.00$
$E(k)$
$D(k)$
k

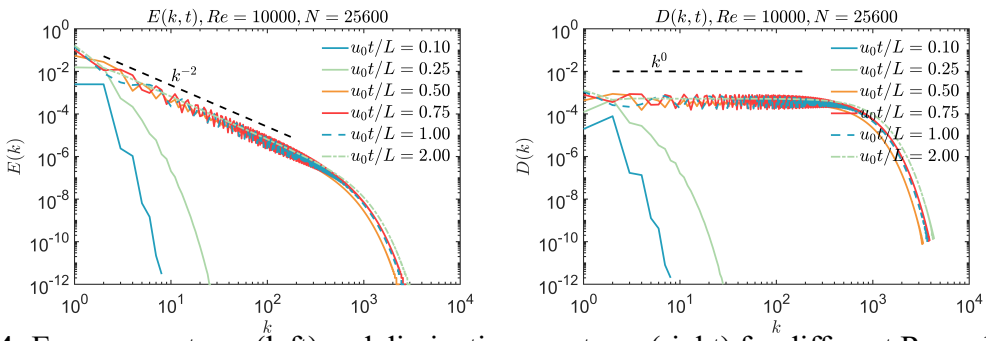

Figure 14. Energy spectrum (left) and dissipation spectrum (right) for differnet Reynolds numbers

With the time evolution, the burgers turbulence exhibits an inertial range wherein low wavenumber flow component transfer energy to the higher ones until to dissipate in the dissipative range, similar to that of real turbulence. The energy spectrum shows an inertial sub-range have a -2 slope, which is different from the real turbulence (Kolmogorov's -5/3 law). The dissipation spectrum shows an inertial sub-range have a 0 slope. The slope law in burgers euqation can be simply derivated by Fourier Transform. With the time evolution, it can be seen that the inertial sub-range evolves toward the correct slope -2; As the Reynolds number increases, the inertial sub-range extends to higher wavenumbers. Dynamics of the small scales in Burgers turbulence is similar but also different from that of the Navier-Stokes because small flow scales are shocks of thickness proportional to the viscosity and are essentially not stochastic.

4.5. The Effect of Unsteady Forcing Term

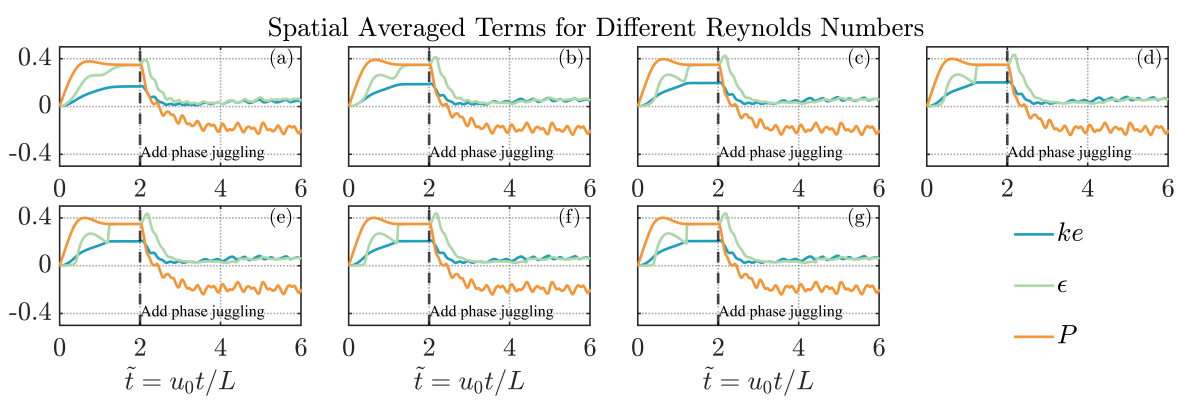

Figure 15. Spatial averaged terms for different Reynolds numbers after add phase juggling; (a) $Re = 100, N = 160$; (b) $Re = 200, N = 320$; (c) $Re = 400, N = 640$; (d) $Re = 800, N = 1280$;(e) $Re = 1600, N = 3200$; (f) $Re = 3200, N = 6400$; (b) $Re = 6400, N = 12800$;

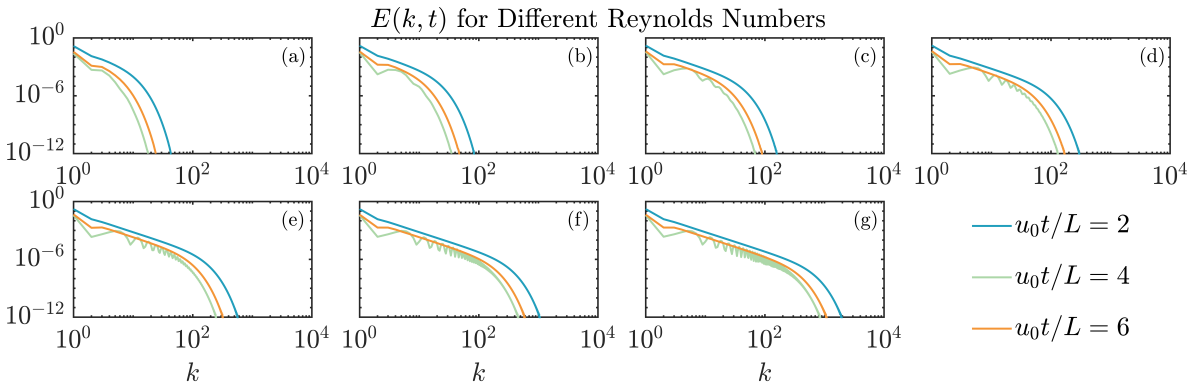

Figure 16. Energy spectrum for different Reynolds numbers after add phase juggling; (a) $Re = 100, N = 160$; (b) $Re = 200, N = 320$; (c) $Re = 400, N = 640$; (d) $Re = 800, N = 1280$;(e) $Re = 1600, N = 3200$; (f) $Re = 3200, N = 6400$; (b) $Re = 6400, N = 12800$;

We add the phase juggling after the velocity reach the steady state.($t = 2s$) According to the time evolution of velocity distribution, we can see that, after adding phase juggling, the initial discontinuity in the middle region starts to gradually move to the left. And a new discontinuity appears on the right side of the computational domain and moves to the right. Finally, the right-moving discontinuity merges with the left-side discontinuity through the periodic boundary conditions, eventually reaching a quasi-steady state.

We plot the spatial averaged terms and energy spectrum for different Re. We found that, after adding the phase juggling, ke, ε, P begin to decrease. Finally, P become negative, while the magnitude of ke and $epsilon$ are approximately same, differing only in phase. In Fig.16, the blue line represents the steady state before adding phase juggling. After phase juggling is introduced, energy transfers from the high wavenumber range to a relatively lower wavenumber range. Once a new balance is reached, the curve becomes smooth again but slightly lower than the original state.

4.6. Discontinuity Thickness for Two Methods

Table 1. The comparison of discontinuity thickness for FDM and FVM

		FDM	FVM
$\delta_{thickness}$	$Re = 1600, N = 1600$	0.002577801262	0.002577790713
	$Re = 3200, N = 6400$	0.000645223453	0.000645223288
	$Re = 6400, N = 12800$	0.000322805245	0.000322805225

The result as shown in Tab.1, the thickness of discontinuity for FVM is slightly smaller than FDM as expected, which manifests the effectiveness of FVM in minimizing numerical dissipation. As the Reynolds number increases, the thickness of the discontinuity decreases progressively.